THE JOURNAL OF BIOLOGICAL CHEMISTRY VOL. 290, NO. 26, pp. 16403–16414, June 26, 2015

Calreticulin and Arginylated Calreticulin Have Different Susceptibilities to Proteasomal Degradation*

Received for publication, November 15, 2014, and in revised form, May 9, 2015 Published, JBC Papers in Press, May 12, 2015, DOI 10.1074/jbc.M114.626127

Victor E. Goitea[1] **and Marta E. Hallak**[2]

From the Centro de Investigaciones en Química Biológica de Córdoba (CIQUIBIC), Consejo Nacional de Investigaciones Científicas y Técnicas, and Departamento de Química Biológica, Facultad de Ciencias Químicas, Universidad Nacional de Córdoba, Córdoba X5000HUA, Argentina

Background: Calreticulin (CRT) retrotranslocated from the endoplasmic reticulum to the cytoplasm is post-translationally arginylated.
Results: Arginylated CRT (R-CRT) has a longer half-life than non-arginylated CRT and displays different ubiquitin dependence.
Conclusion: CRT and R-CRT differ in their susceptibility to proteasomal degradation.
Significance: Arginylation is not required for proteasomal degradation of CRT, although R-CRT displays ubiquitin modification.

Post-translational arginylation has been suggested to target proteins for proteasomal degradation. The degradation mechanism for arginylated calreticulin (R-CRT) localized in the cytoplasm is unknown. To evaluate the effect of arginylation on CRT stability, we examined the metabolic fates and degradation mechanisms of cytoplasmic CRT and R-CRT in NIH 3T3 and CHO cells. Both CRT isoforms were found to be proteasomal substrates, but the half-life of R-CRT (2 h) was longer than that of cytoplasmic CRT (0.7 h). Arginylation was not required for proteasomal degradation of CRT, although R-CRT displays ubiquitin modification. A CRT mutant incapable of dimerization showed reduced metabolic stability of R-CRT, indicating that R-CRT dimerization may protect it from proteasomal degradation. Our findings, taken together, demonstrate a novel function of arginylation: increasing the half-life of CRT in cytoplasm.

Post-translational modifications (PTMs)[3] of proteins are essential for regulation of subcellular localization, function, structure, and complex formation capability (1–3). Arginylation is a PTM mediated by arginyl-tRNA-protein transferase (Ate1), which transfers Arg from arginyl-tRNA onto proteins that have an acidic amino acid or Cys as the N-terminal residue (4–6). Many proteins are arginylated *in vivo* (7, 8), and this PTM plays key roles in a variety of physiological processes (3) including cell adhesion (9, 10), apoptosis (11), and cellular stress (7, 12, 13).

Calreticulin (CRT) is localized mainly in the endoplasmic reticulum (ER) and has multiple functions within and outside the ER (14–16). Our group was the first to demonstrate the retrotranslocation of CRT from the ER (ER-CRT) to the cytoplasm under conditions that promote reduction of cytoplasmic Ca^{2+} levels (7, 12). In the cytoplasm, CRT is post-translationally arginylated *in vivo* by Ate1 (7, 12). Arginylated CRT (R-CRT) is not detectable in the ER lumen (7), consistently with the cytosolic and nuclear localization of Ate1 (17). We showed that arginylation of CRT is essential for its association with stress granules (SGs) and promotes its dimerization (7, 13). Apoptosis induction is associated with an increased R-CRT level at the cell surface (11). Surface exposure of CRT on tumor cells has been suggested to promote their uptake by phagocytes (18). The effects of CRT arginylation on its cytoplasmic functions and final destination remain to be elucidated.

According to the "N-end rule," which relates the half-life of a protein to the identity of its N-terminal residue, N-terminal Asp and Glu are secondary destabilizing residues that function through their arginylation to yield the primary destabilizing residue Arg (19). Arginylation in turn promotes protein recognition by specific E3 ubiquitin (Ub)-protein ligases that polyubiquitinate proteins on internal Lys residues (20). Proteasomal degradation depends in most cases on Ub conjugation (ubiquitination). However, a significant subset of proteins displays ubiquitination-independent turnover (21), which is not surprising in view of the co-existence of several types of proteasomal complexes in eukaryotic cells (22). The possible role of CRT as a substrate for proteasomal degradation is controversial (23–25). The degradation mechanism of R-CRT remains unknown.

To assess the effect of CRT arginylation on its stability, we studied the degradation of cytoplasmic CRT (cyt-CRT) and R-CRT in fibroblasts and CHO cells, including the roles of proteasomes, Ub modification, and dimer formation in this process. We found that arginylated and non-arginylated isoforms

* This work was supported by grants from the Agencia Nacional de Promoción Científica y Technologica (PICT 2012-1979), Consejo Nacional de Investigaciones Científicas y Técnicas, and La Secretaría de Ciencia y Tecnología, Universidad Nacional de Córdoba. The authors declare that they have no conflicts of interest with the contents of this article.
[1] Recipient of a fellowship from Consejo Nacional de Investigaciones Científicas y Técnicas.
[2] A member of the Research Career of Consejo Nacional de Investigaciones Científicas y Técnicas. To whom correspondence should be addressed: Haya de la Torre y Medina Allende X5000HUA, Córdoba, Argentina. Tel.: 54-351-5353855; Fax: 54-351-4334074; E-mail: mhallak@fcq.unc.edu.ar.
[3] The abbreviations used are: PTM, post-translational modification; CRT, calreticulin; R-CRT, arginylated calreticulin; cyt-CRT, cytoplasmic CRT; Ate1, arginyl-tRNA protein transferase; SG, stress granule; ER, endoplasmic reticulum; Ub, ubiquitin; CHX, cycloheximide; Tg, thapsigargin; Ab, antibody; pAb, polyclonal antibody; EGFP, enhanced green fluorescent protein.

of CRT are proteasomal substrates that follow different degradation pathways: one dependent on and the other independent of Ub modification. Biochemical analysis showed that CRT arginylation leads to ubiquitination of R-CRT isoforms but reduces turnover rate. Our finding that arginylation stabilizes CRT is in contrast to the traditional view of arginylation as a destabilizing factor.

Experimental Procedures

Cell Culture—All cell lines were cultured in a humidified incubator with 5% CO_2 in standard DMEM (Life Technologies) supplemented with 10% (v/v) FBS (Life Technologies), 4 mM L-glutamine (Sigma), 200 units/ml penicillin, and 100 μg/ml streptomycin (Life Technologies). ATE1$^{-/-}$ and ATE1$^{+/+}$ mouse EF (embryonic fibroblast) cell lines were kindly provided by Dr. A. Kashina (Dept. of Animal Biology/Biochemistry, University of Pennsylvania, Philadelphia, PA). CRT$^{-/-}$ and CRT$^{+/+}$ mouse EF cell lines were a gift from Dr. M. Michalak (Dept. of Biochemistry, University of Alberta, Edmonton, Canada).

Plasmids—For cloning of pEGFP-CRT (with signal peptide) we digested pEYFP-CRT plasmid (12) with EcoRI and KpnI endonucleases and cloned the fragment containing the coding sequence of human full-length CRT into pEGFP-N1 expression vector (Clontech Laboratories; Palo Alto, CA). To express mature CRT (without signal peptide) in cytoplasm, we adapted a strategy described previously for GFP (26). In brief, DNAs encoding Ub fused to mature human CRT (Ub-CRT) or R-CRT (Ub-R-CRT) were cloned in pEGFP-N1 expression vector. The Ub moiety was cleaved in cytoplasm by Ub-C-terminal hydrolases to release mature CRT with exposed N-terminal Glu or Arg, as confirmed by Western blotting (Fig. 3). For cloning of pEGFP-Ub-CRT and pEGFP-Ub-R-CRT cDNAs, the coding sequences of Ub-CRT and R-CRT were amplified by PCR from pHUE-CRT-FLAG and pHUE-R-CRT-FLAG expression vectors, respectively (11). The forward primer (same for both amplification reactions) contained an EcoRI restriction site (underlined), a Kozak sequence (boldfaced), and the Ub sequence (italicized): 5′-CCGGAATTC**CCCGCCGCCACC*-ATGC***AGATCTTTGTGAAGACCCTCACTGG*-3′. The reverse primer (the same for both amplification reactions) contained a KpnI restriction site (underlined) and the CRT sequence (italicized): 5′-CGGGGTACC*CCCAGCTCGTCCTTGGCCTG GCC*-3′. The PCR products were digested with EcoRI and KpnI endonucleases and cloned into pEGFP-N1 expression vector. All constructs were confirmed by DNA sequencing.

Mutant Construction and Site-directed Mutagenesis—For generation of the pEGFP-C146A-CRT mutant, we digested the pEYFP-C146A-CRT plasmid (13) with EcoRI and KpnI endonucleases and cloned the fragment containing the coding sequence of human full-length C146A-CRT into pEGFP-N1 expression vector.

For cloning of the pEGFP-Ub-E1V-CRT mutant, we used the site-specific mutagenesis method with overlap extension (27). Construction of the E1V mutation (numbering starts from the mature CRT) required two mutagenic primers, two flanking oligonucleotides, and three PCR. One pair of primers was used to amplify the DNA containing the mutation site together with downstream sequences. The reverse primer contained the mutation (underlined and boldfaced) introduced into the wild-type (WT) template cDNA of Ub-CRT: 5′-AAGTAGACGGC-AGGC**A**CTCCACCGCGGAGGCGCAACACC-3′. The forward primer (F2) was the same as for the Ub-CRT WT sequence described under "Plasmids" (above) and contained an EcoRI restriction site, a Kozak sequence, and the Ub sequence. The second pair of primers was used to amplify the DNA that contained the mutation site together with upstream sequences. The forward primer of this pair contained the mutation (underlined and boldfaced) introduced into the template DNA and was complementary to reverse primer: 5′-GCCTCCGCGGT-GGAG**T**GCCTGCCGTCTACTTCAAGGAGC-3′. The reverse primer (R2) was the same as for the Ub-CRT WT sequence described under "Plasmids" (above) and contained a KpnI restriction site and the CRT sequence. To amplify the overlapping DNA fragments, both sets of primers were used in two separate amplification reactions. The mutation of interest was located in the overlap region and, therefore, in both sets of the resulting amplified fragments. The full-length Ub-E1V-CRT DNA was amplified by a third PCR, mixing the overlapping fragments and using primers F2 and R2 that bind to the 3′ and 5′ extremes of the initial fragments, respectively. The PCR products were digested with EcoRI and KpnI endonucleases and cloned into pEGFP-N1 expression vector. All constructs were confirmed by DNA sequencing.

Cell Transfection—CHO cells were transfected using Lipofectamine 2000 and Opti-MEM (Life Technologies) according to the manufacturer's instructions. ATE1$^{-/-}$ and CRT$^{-/-}$ cells were transfected in Opti-MEM with pEGFP-Ub-CRT or pEGFP-Ub-R-CRT and pEGFP-CRT or pEGFP-C146A-CRT, respectively, using Lipofectamine LTX with Plus reagent (Life Technologies).

Inhibitor Treatments—Inhibitors (Sigma) were used at the following concentrations: MG132 10 μM, cycloheximide (CHX) 50 μg/ml, thapsigargin (Tg) 2 μM.

Establishment of Stable Cell Lines—CHO cells were transfected with pEGFP-Ub-CRT, pEGFP-Ub-R-CRT, or pEGFP-Ub-E1V-CRT. Stably transfected cell lines were selected in the presence of 0.5 mg/ml G418 (Phytotechnology Laboratories; Overland Park, KS). To obtain stable cell lines that uniformly expressed CRT-EGFP, R-CRT-EGFP, or E1V-CRT-EGFP, we isolated populations with intermediate levels of EGFP expression by fluorescence-activated cell sorting (FACS Aria IIu; BD Biosciences) after treatment with MG132 (Sigma).

Immunofluorescence—Cells were grown on glass coverslips to 60% confluence, and immunofluorescence was stimulated as described previously (7, 13). Nuclei were stained with DAPI.

Protein Half-life Assay—Stable CHO cell lines expressing CRT-EGFP, R-CRT-EGFP, or E1V-CRT-EGFP were treated for 9 h with MG132 to cause accumulation of EGFP fusion proteins. Alternatively, ATE1$^{-/-}$ cells were transfected transiently with pEGFP-Ub-CRT or pEGFP-Ub-R-CRT, cultured for 6 h, and treated with MG132 for the indicated times in the Figs. 8 and 9 legends. In both cases cells were washed 4 times, cultured for 1 h to allow diffusion of the inhibitor, and washed again. CHO cells were incubated for various durations with CHX or MG132. Proteins were separated by SDS-PAGE, and levels of

EGFP fusion proteins and R-CRT were monitored by Western blotting.

In Vivo Ubiquitination Assay—To increase Ub levels and the sensitivity of Ub detection, CHO cells were transfected transiently with pcDNA3-HA-Ub or co-transfected with pcDNA3-HA-Ub and pEGFP-Ub-R-CRT or pEGFP-Ub-E1V-CRT. Six hours after transfection, cells were cultured with proteasome inhibitor for 16–18 h. Cell lysates were prepared using lysis buffer (50 mM Tris-HCl, pH 7.5, 150 mM NaCl, 1% Nonidet P-40, 0.1% deoxycholate) plus 5 mM iodoacetamide, 5 mM *N*-ethylmaleimide, 10 μM MG132, and 1:100 protease inhibitor mixture (Calbiochem) to inhibit deubiquitinating enzymes and proteases and then sonicated briefly on ice. The remaining steps were performed at 4 °C. Lysates were precleared by centrifugation at 13,000 × *g* for 10 min, and the supernatants were subjected to immunoprecipitation for EGFP. The protein samples were separated by SDS-PAGE and immunoblotting with anti-HA and anti-GFP antibodies (Abs).

Immunoprecipitation—All steps were performed at 4 °C. Cell lysates were incubated on an orbital shaker with 50 μl of protein G-Sepharose beads (GE Healthcare) for 2 h to reduce nonspecific protein binding. Beads were pelleted for 20 s at 2300 rpm. To immunoprecipitate EGFP fusion proteins, supernatants were incubated with 2 μl of anti-GFP for 1 h, added with 50 μl of protein G-Sepharose beads, and incubated on a rocker for 4 h. Protein G-Sepharose·Ab complexes were pelleted at 2300 rpm for 20 s and washed twice in 500 μl of lysis buffer and once in washing buffer (50 mM Tris-HCl, pH 7.5, 250 mM NaCl, 0.1% Nonidet P-40, 0.05% deoxycholate). Protein G-Sepharose·Ab complexes were resuspended in sample buffer 2×. Total cell lysate and bound and unbound fractions were subjected to SDS-PAGE, and proteins were transferred to nitrocellulose membrane for immunoblotting.

Cell Viability Assay—Cell viability was determined by the colorimetric technique using resazurin (28) (Sigma). In each assay, 10,000 cells were plated per well in 96-well plates. Cells were treated at various intervals (see Fig. 6*A*) with 10 μM MG132 or vehicle. After this treatment, 2 μl of 1 mg/ml resazurin solution were added to 200 ml of medium per well. Plates were incubated at 37 °C for 4 h, and the optical density was measured at 600 nm wavelength in a FL X800 Microplate Reader (BioTek Instruments, Inc.)

Assessment of Cell Death—Cells/sample were collected as in López Sambrooks *et al.* (11). Briefly, cells were washed in PBS, pelleted, and resuspended in buffer (10 mM HEPES/NaOH, pH 7.4, 140 mM NaCl, 2.5 mM $CaCl_2$) containing propidium iodide to identify dead cells. Cells were analyzed by flow cytometry on a FACSCantoII cytometer (BD Biosciences) using FlowJo software.

Western Blotting—Proteins from cell lysates and immunoprecipitates were resolved by SDS-PAGE (29) and transferred onto nitrocellulose membranes (Potran BA 83, Whatman; Sanford, FL) (30). The filters were blocked at room temperature for 1 h in PBS supplemented with 5% nonfat dry milk. Blots were incubated with primary Abs to detect the expression of EGFP (1:2,500, mouse monoclonal anti-GFP Ab, Roche Applied Science), R-CRT (1:100, rabbit anti-R-CRT polyclonal antibody (pAb), custom made by Eurogentec; Seraing, Belgium) (7, 12), β-actin (1:20,000, mouse monoclonal anti-β-actin Ab; Sigma), and HA-Ub (1:1,500, rabbit monoclonal anti-HA Ab, Cell Signaling; Boston, MA)) overnight on a rocker at 4 °C. After washing, blots were incubated for 1 h at room temperature with secondary Abs: InfraRedDye-680 goat anti-mouse Ab (1:25000, LI-COR Biosciences; Lincoln, NE) and IRD-800 goat anti-rabbit Ab (1:15000, LI-COR). The immunodetected proteins were visualized by an Odyssey IR-imaging system (LI-COR).

Imaging and Image Analysis—Images were acquired on a laser scanning confocal microscope (FluoView 1000; Olympus; Center Valley, PA) with a 60× oil immersion lens, NA 1.42. At least 200 cells were examined for each condition. Fiji software was used to measure cell fluorescence and calculate the corrected total cell fluorescence with correction for background fluorescence. Blot images acquired from the Odyssey IR-imaging system were analyzed using Odyssey Application Software v.2.1 (LI-COR).

Statistical Analysis—Significance was tested by one-way or two-way analysis of variance using the GraphPad Prism 5.01 program (GraphPad Software). One-way and two-way analysis of variance was followed, respectively, by the Newman-Keuls and Bonferroni multiple comparison test. Differences were considered significant for $p < 0.05$. Half-lives were calculated using nonlinear regression and one-phase decay analysis.

Results

R-CRT Accumulation Results from Proteasomal Inhibition—Arginylation is considered a primary destabilizing residue according to the N-end rule for targeting proteins to proteasomal degradation (19). To evaluate the role of arginylation in removal of intracellular R-CRT, we incubated NIH 3T3 cells in the presence of a potent reversible proteasome inhibitor (MG132) and measured the cellular content of endogenous cytoplasmic R-CRT by immunofluorescence at intervals using anti-R-CRT Ab. This antibody specifically recognizes endogenous R-CRT (7). After 1 h of MG132 treatment, the R-CRT level was twice as high as that of control (non-treated) cells ($p < 0.001$) (Fig. 1, *A* and *B*). After 2 h of treatment, the level was slightly ($p < 0.05$) higher than that at 1 h (Fig. 1, *A* and *B*). There was a possibility that these findings resulted from inhibition of cysteine protease by MG132 (31). We, therefore, performed similar studies with lactacystin, an irreversible specific proteasome inhibitor that does not affect cysteine proteases (32), and obtained similar results (Fig. 2).

MG132 inhibits proteasomal degradation and also leads to a heat-shock response that induces expression of ER chaperones (33). Whether MG132 promotes retrotranslocation of ER proteins is unknown. The increase of R-CRT after proteasome inhibition could, therefore, be due to either increased CRT synthesis or retrotranslocation. Our subsequent experiments were designed to distinguish between these two possibilities.

We showed previously that R-CRT content increases when cells are treated with an ER stressor (Tg) (7, 12). To determine whether such an R-CRT increase is affected by proteasomal inhibition, NIH-3T3 cells were treated with Tg in the presence and absence of MG132. R-CRT level in the Tg-treated cells was increased to a similar degree regardless of MG132 treatment (Fig. 1, *C* and *D*). However, when Tg was removed after 20 min

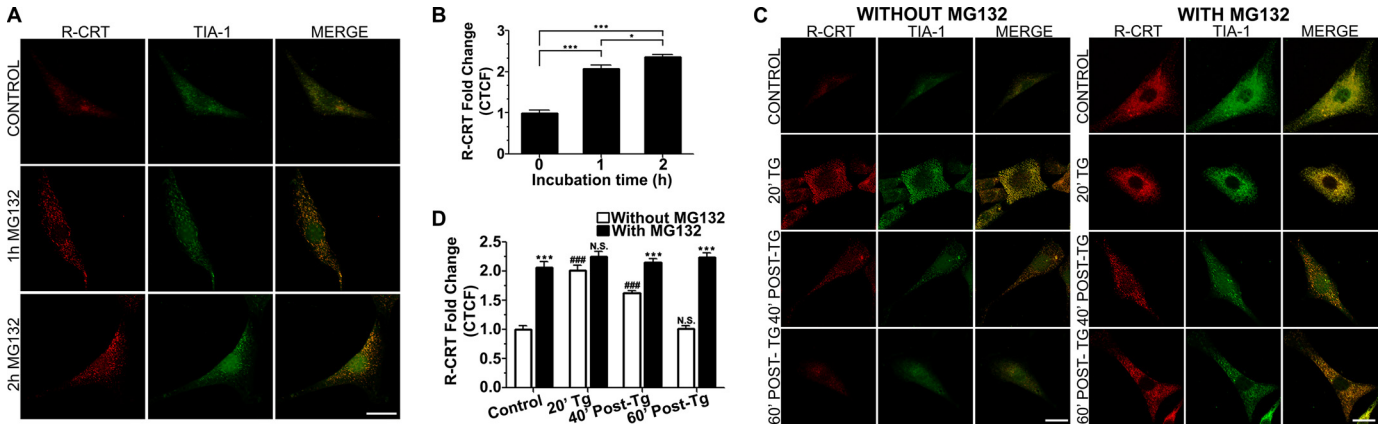

FIGURE 1. **Proteasome inhibition in NIH 3T3 cells results in R-CRT accumulation in SGs.** *A*, NIH 3T3 cells were incubated with MG132 (10 μM) for 1 and 2 h (control: 0 h treatment). *B*, quantification of fluorescence intensity in immunofluorescence (*A*). Data are shown as the mean ± S.E. *, $p < 0.05$; ***, $p < 0.001$ for comparison with control. *C*, cells incubated in the absence or presence of MG132 (10 μM) and treated with Tg (2 μM) for 20 min (*20′ TG*) were analyzed 40 and 60 min after Tg removal (*40′ Post-TG* and *60′ Post-TG*). *D*, quantification of fluorescence intensity in immunofluorescence data (*C*). The corrected total cell fluorescence was expressed as fold change value relative to control (0 h). Data are shown as the mean ± S.E. ***, $p < 0.001$ for intragroup comparison; *i.e. black bar versus white bar* within each of the four experimental groups. ###, $p < 0.001$ for intergroup comparison with control (0 h) group; *i.e. white* or *black bar* of 20′ TG, 40′ Post-TG, or 60′ Post-TG group *versus* the corresponding bar of the control group. Results shown are representative of 200 cells from at least three separate experiments for each condition. *Scale bars*, 20 μm. *N.S.*, not significant. Cells were analyzed by double immunofluorescence using anti-R-CRT and SG marker anti-TIA-1 pAbs. Co-localization of proteins was monitored by confocal microscopy. SG formation was observed upon MG132 treatment, and R-CRT was found to be co-localized with SGs as shown by yellow pseudo-color in the merge images.

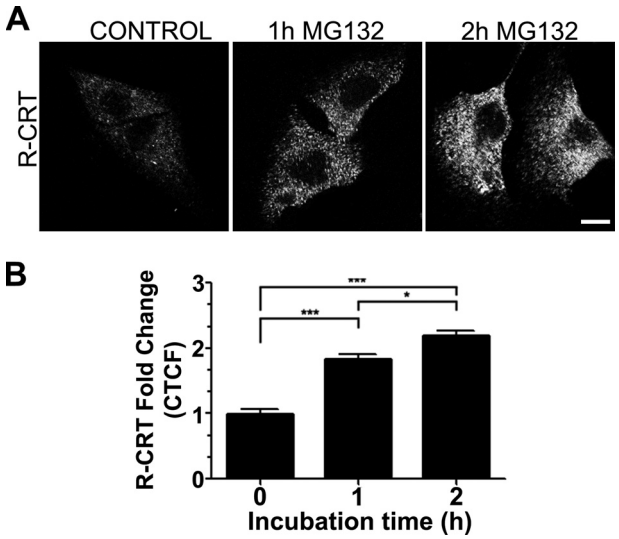

FIGURE 2. **R-CRT accumulation in the presence of lactacystin.** *A*, NIH 3T3 cells were incubated with 10 μM lactacystin (*LACTA*) for 1 or 2 h (*CONTROL*: 0 h). Cells were analyzed by immunofluorescence using anti-R-CRT pAb. *B*, quantification of fluorescence intensity in immunofluorescence data (*A*). Corrected total cell fluorescence was expressed as -fold change value relative to control. Results shown are representative of 200 cells from at least three separate experiments for each condition. *Scale bar*, 10 μm. Data are shown as the mean ± S.E. *, $p < 0.05$; ***, $p < 0.001$ for comparison with control.

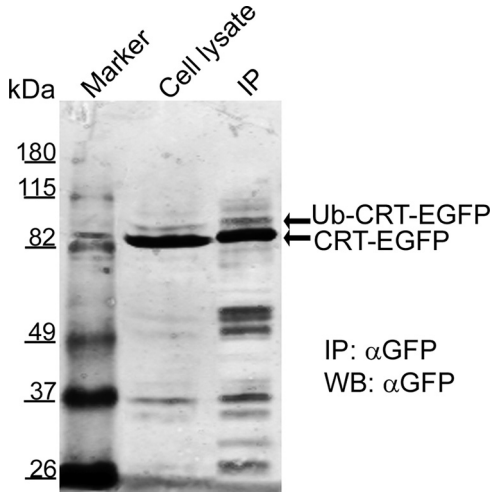

FIGURE 3. **Cytoplasmic expression of CRT.** CHO cells transfected with Ub-CRT-EGFP were incubated with MG132 (10 μM) for 18 h. Cell lysates were immunoprecipitated (*IP*) with anti-GFP Ab followed by immunoblotting (*WB*) with anti-GFP. Polypeptides with sizes corresponding to the cleaved product and uncleaved precursor are indicated. A band corresponding to the Ub-CRT-EGFP precursor was detected only in the treated cells after prolonged exposure of the blots.

of treatment, the increased R-CRT level was maintained only in cells treated with MG132 for 40 or 60 min (Fig. 1, *C* and *D*). The R-CRT level resulting from treatment with Tg alone was not increased by the addition of MG132 (Fig. 1*D*: *20′ Tg, white versus black bar*), indicating that MG132 did not activate CRT retrotranslocation. The sustained increase of R-CRT in the presence of MG132 after Tg removal was, therefore, due to impaired proteasomal degradation. Because cyt-CRT accumulation results from retrotranslocation of stored ER-CRT, it is not possible to evaluate CRT degradation by using a protein synthesis inhibitor to block CRT synthesis. Taken together, these findings suggest that CRT is arginylated after retrotranslocation from the ER to the cytoplasm (7, 12), and R-CRT is then removed by the proteasomal degradation system.

Cyt-CRT Is Degraded Rapidly by Proteasomes in an Arginylation-independent Manner—To determine whether arginylation of CRT is required for its proteasomal degradation, we evaluated CRT degradation under conditions that precluded N-terminal arginylation and analyzed proteasomal degradation of CRT, R-CRT, and a non-arginylatable CRT (E1V-CRT) expressed directly in the cytoplasm. Stable CHO cell lines expressing three chimeric proteins (Ub-CRT-EGFP, Ub-R-CRT-EGFP, Ub-E1V-CRT-EGFP) were used. Cleavage of the Ub moiety by cellular C-terminal hydrolases was confirmed by Western blotting (Fig. 3). Under immunofluorescence micros-

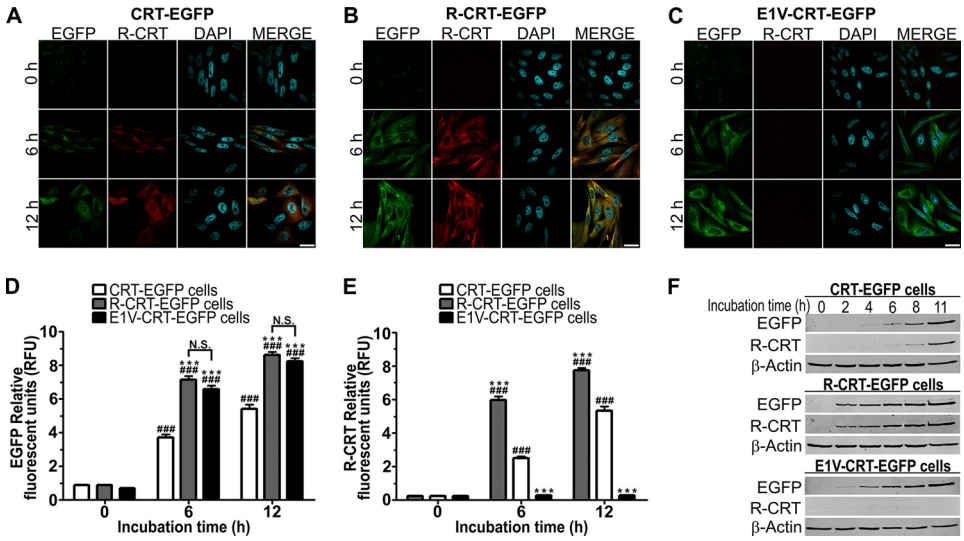

FIGURE 4. **cyt-CRT with various N termini are rapidly degraded by proteasomes.** Stably transfected cells expressing CRT-EGFP (*A*), R-CRT-EGFP (*B*), or E1V-CRT-EGFP (*C*) were incubated with MG132 (10 μM) for various durations and analyzed by triple immunofluorescence for detection of EGFP emission using anti-R-CRT pAb and DAPI. Merge images for EGFP emission and anti-R-CRT Ab are shown in the corresponding panels. *Scale bars*, 20 μm. Quantification of fluorescence intensity in immunofluorescence data of EGFP emission (*D*) or anti-R-CRT Ab (*E*) was expressed in relative fluorescence units (*RFU*). Data are shown as the mean ± S.E. ***, $p < 0.001$ for intragroup comparison; *i.e. gray* (or *black*) *bar versus white bar* within each of the three experimental groups. ###, $p < 0.001$ for intergroup comparison with 0 h group; *i.e. white*, *gray*, or *black bar* of 6-h or 12-h group *versus* the corresponding *bar* of the 0 h group. *N.S.*, not significant. Results are representative of 180 cells from at least three separate experiments for each condition. *F*, immunoblotting analysis of CRT-EGFP, R-CRT-EGFP, and E1V-CRT-EGFP content for the indicated MG132 incubation times.

copy, stably transfected cells showed EGFP fluorescence levels slightly higher than the autofluorescence of nontransfected cells, most likely because of rapid degradation of the expressed proteins (Fig. 4, *A*–*C*). In cells treated with MG132, CRT-EGFP, R-CRT-EGFP, and E1V-CRT-EGFP, levels increased at different times (Fig. 4*D*). Immunocytochemical analysis (with an anti-R-CRT Ab) of R-CRT-EGFP- and CRT-EGFP-transfected cells treated with MG132 revealed similar accumulations of R-CRT (Fig. 4*E*). In contrast, R-CRT was not detected in E1V-CRT-EGFP-transfected cells, consistent with the presumed inability of N-terminal Val to incorporate Arg (Fig. 4, *C*–*E*). Although all three variants showed CRT accumulation in the presence of MG132, Western blotting with anti-GFP Ab revealed differences in their accumulation rates (Fig. 4*F*). An increase of R-CRT-EGFP expression was observed after 2 h of MG132 treatment, whereas cells expressing non-arginylatable E1V-CRT-EGFP or arginylatable CRT-EGFP required 4 and 6 h of MG132 treatment, respectively (Fig. 4*F*). In CRT-EGFP-expressing cells treated with MG132, protein accumulation was detected with anti-GFP at essentially the same time that R-CRT accumulation was detected by Western blotting with anti-R-CRT Ab (Fig. 4*F*). Taken together, these findings indicate that proteasome inhibition results in accumulation of R-CRT-EGFP, CRT-EGFP, and E1V-CRT-EGFP and suggested that (i) CRT arginylation is not required for its degradation, and (ii) R-CRT-EGFP and E1V-CRT-EGFP are less susceptible to proteasome degradation than is CRT-EGFP.

Effect of the N-terminal Amino Acid on CRT Half-life—The observed accumulation of CRT-EGFP, R-CRT-EGFP, and E1V-CRT-EGFP after MG132 treatment could be explained by differential rates of synthesis (34). To evaluate this possibility, we determined the half-life of each protein in the presence of the protein synthesis inhibitor CHX. Stably transfected cells as described in the preceding section were incubated with MG132 to accumulate the corresponding protein (CRT-EGFP, R-CRT-EGFP, E1V-CRT-EGFP), MG132 was removed, cells were incubated further with CHX, and EGFP clearances were determined at various times by Western blotting (Fig. 5*A*). Clearance was more pronounced for CRT-EGFP than for R-CRT-EGFP or E1V-CRT-EGFP (Fig. 5, *A* and *C*). No changes in clearance were observed when cells were incubated with CHX in the presence of MG132 (Fig. 5, *B* and *D*). Half-lives in the presence of CHX were ~1.3 h for the mixture of CRT-EGFP and R-CRT-EGFP present in CRT-EGFP cells, ~0.7 h for the non-arginylated CRT-EGFP, ~2.0 h for R-CRT-EGFP, and ~4.8 h for E1V-CRT-EGFP (Fig. 5*E*); *i.e.* the half-life of non-arginylated CRT-EGFP was 65% shorter than that of R-CRT-EGFP and 85% shorter than that of E1V-CRT-EGFP. The half-life of R-CRT from CRT-EGFP and R-CRT-EGFP, as determined using anti-R-CRT antibody, was ~2.0 h (Fig. 5*F*), a similar value than that obtained employing anti-GFP antibody (Fig. 5, *C* and *E*).

MG132 has been reported to induce apoptosis in some cases (35). It is, therefore, conceivable that this inhibitor affects CRT levels indirectly via some apoptosis-related mechanism.

To test this possibility, we cultured CHO cells expressing CRT-EGFP, R-CRT-EGFP, or E1V-CRT-EGFP in the presence of MG132 and analyzed cell viability by the colorimetric resazurin assay. No changes were observed in viability at least up to 24 h of MG132 treatment (Fig. 6*A*). Moreover, no significant increase in cell death was detected by flow cytometry of propidium iodide-stained cells at the times studied (Fig. 6*B*).

These findings demonstrate that CRT-EGFP, R-CRT-EGFP, and E1V-CRT-EGFP undergo proteasomal degradation and that arginylation of CRT is not required for its proteasomal degradation. Because CRT-EGFP is arginylated by Ate1 and some CRT-EGFP remains arginylation-free (Fig. 7), the half-life of the mixture of non-arginylated CRT-EGFP and R-CRT-

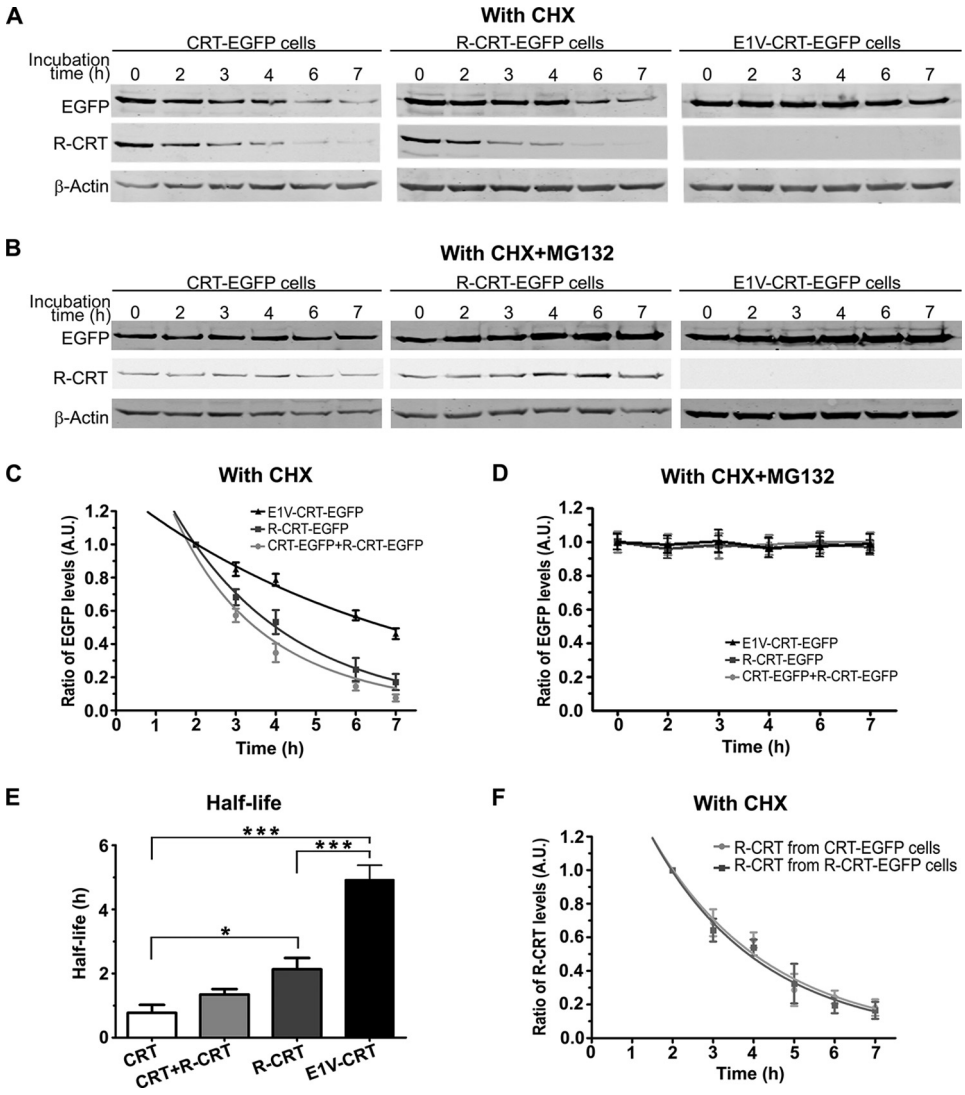

FIGURE 5. **Non-arginylated CRT has a shorter half-life than arginylated CRT and non-arginylatable CRT.** Stably transfected cells expressing CRT-EGFP, R-CRT-EGFP, or E1V-CRT-EGFP were treated with MG132 to cause accumulation of these proteins. MG132 was removed, cells were incubated in the presence of CHX (*A*) or CHX+MG132 (*B*), and contents of CRT-EGFP, R-CRT-EGFP, and E1V-CRT-EGFP were analyzed at the indicated incubation times by immunoblotting with anti-GFP, anti-R-CRT, and anti-β-actin Abs. The Western blots shown are representative of seven independent experiments. *C* and *D*, intensities of EGFP bands relative to β-actin were measured, expressed as arbitrary units (*A.U.*) and plotted as a fraction of band intensity at 2 h. To make possible determination of half-lives in the linear range, we did not consider the initial band intensity (0 h), because this signal is saturated and cannot be used for half-life calculation. *E*, half-lives were determined in the linear range (2 h through 7 h as shown in *A–D*). Estimated half-lives of R-CRT-EGFP and E1V-CRT-EGFP were extrapolated by non-linear regression from a one-phase exponential decay curve fitted to the data points in *C*. Estimated half-life of non-arginylated CRT-EGFP was calculated by non-linear regression from a two-phase exponential decay curve fitted to the data points of the CRT/R-CRT mixture present in CRT-EGFP cells, in *C*. The constraints used for the two-phase exponential decay curve were: (i) half-life of R-CRT (2 h); (ii) percentage of initial non-arginylated CRT-EGFP (40%; Fig. 7). Values shown are the mean ± S.E. of seven independent experiments. *, $p < 0.05$; ***, $p < 0.001$. *F*, intensities of R-CRT bands relative to β-actin from CRT-EGFP and R-CRT-EGFP cells in the presence of CHX were measured, expressed as arbitrary units (*A.U.*), and plotted as a fraction of band intensity at 2 h. The estimated half-lives of R-CRT from CRT-EGFP and R-CRT-EGFP cells are the same and consistent with those calculated for R-CRT-EGFP cells using anti-GFP Ab (2 h).

EGFP is presumed to lie between that of R-CRT-EGFP and E1V-CRT-EGFP. However, the degradation of the mixture of non-arginylated CRT-EGFP and R-CRT-EGFP is faster than that of R-CRT-EGFP or E1V-CRT-EGFP (Fig. 5*E*), indicating that non-arginylated CRT-EGFP should be degraded more efficiently.

Degradation of R-CRT and CRT in Cells Lacking Ate1—The mutation introduced into CRT for preparation of E1V-CRT may, in addition to preventing its arginylation, induce conformational changes in the protein. To test this possibility, we examined CRT-EGFP degradation in ATE1$^{-/-}$ cells (9, 36). These cells were transfected with Ub-CRT-EGFP or Ub-R-CRT-EGFP and treated with MG132 for 18 h to allow cytoplasmic accumulation of CRT-EGFP or R-CRT-EGFP. MG132 was removed, cells were cultured with CHX for 2 h, and protein expression was analyzed by Western blotting. In agreement with the results shown in Fig. 5, CRT-EGFP and R-CRT-EGFP were decreased by treatment with CHX alone but unaffected by treatment with CHX plus MG132 (Fig. 8, *A* and *B*). The CHX-induced decrease was significantly smaller (<40%; $p < 0.05$) for R-CRT-EGFP- *versus* CRT-EGFP-expressing cells (Fig. 8*B*). The simplest interpretation of these findings is that arginylation of CRT impairs its degradation and that different proteasomal pathways are involved in the degradation of CRT *versus* R-CRT.

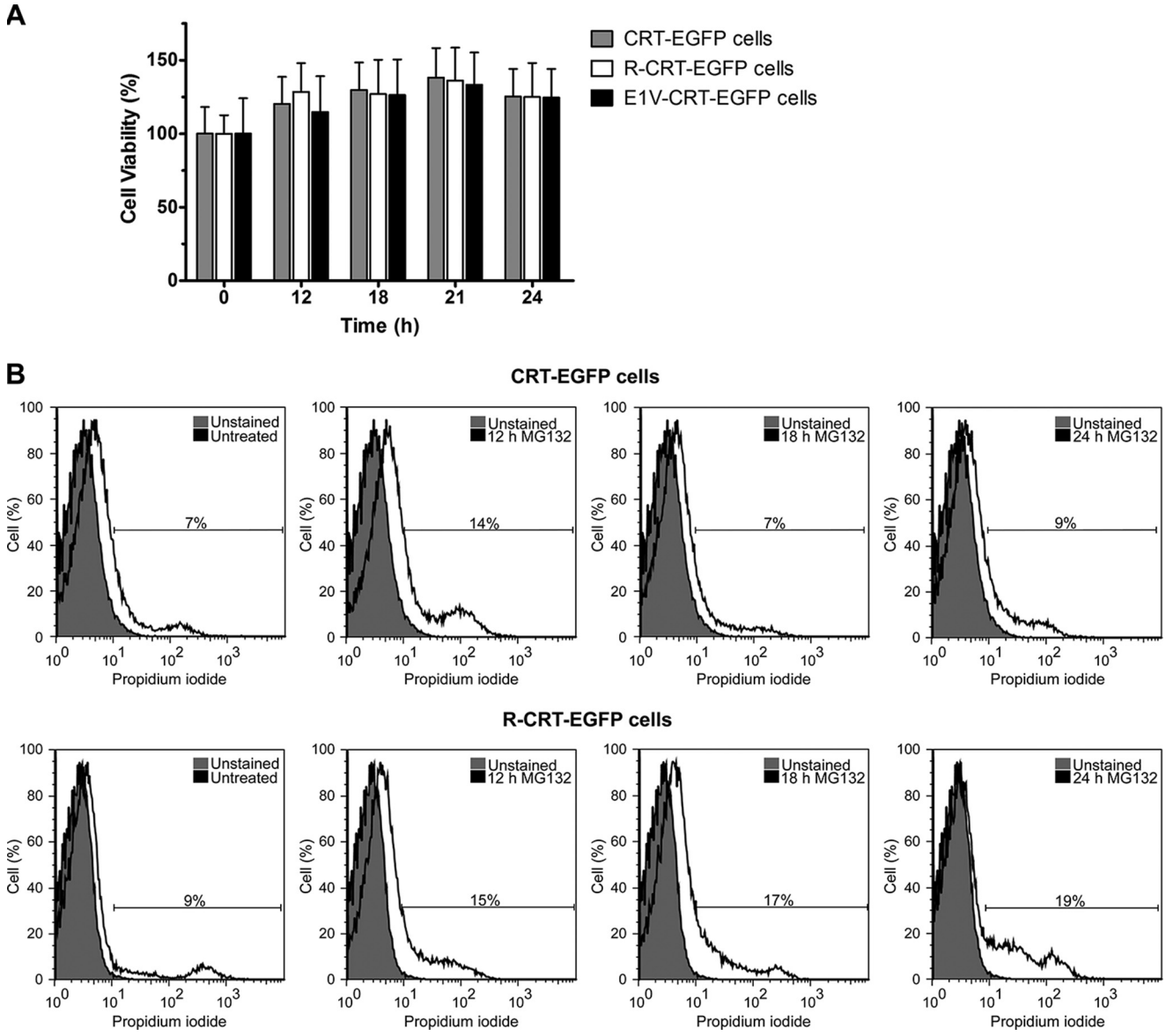

FIGURE 6. **Viability and apoptosis control upon MG132 treatment.** *A*, viability of cells expressing R-CRT-EGFP, CRT-EGFP, or E1V-CRT-EGFP, assessed by the reduction of resazurin at various intervals (12, 18, 21, 24 h) of treatment with 10 μM MG-132. Data are the means ± S.D. ($n = 6$). All comparisons were not significant at $p > 0.05$. *B*, flow cytometry histograms of cells stably expressing CRT-EGFP or R-CRT-EGFP stained with propidium iodide at various intervals (12, 18, 24 h) of treatment with 10 μM MG132. Values of 100% correspond to 50,000 cells. The data shown are the means of three independent experiments. MG132 treatment for 24 h with a dose of 10 μM did not induce apoptosis. The slight induction of apoptosis in R-CRT-EGFP cells at 24 h of MG132 treatment may have been due to accumulation of pro-apoptotic R-CRT in the plasma membrane (11).

To rule out the possibility that EGFP contributes to the degradation of these variants, ATE1$^{-/-}$ cells were transfected with Ub-CRT-FLAG or Ub-R-CRT-FLAG and treated with MG132 for 12 h to allow cytoplasmic accumulation of CRT-FLAG or R-CRT-FLAG. MG132 was removed, cells were cultured with CHX for 1 or 2 h, and protein level was analyzed by Western blotting. Results for proteins fused with FLAG *versus* EGFP at the C terminus of isoforms were similar (Fig. 9, *A–D*), indicating that the CRT sequence encloses the signal for degradation and that the signal is not affected by EGFP fusion at the C terminus.

R-CRT-EGFP Is Degraded by the Ub Proteasome System—The finding that arginylatable CRT-EGFP is degraded more rapidly than are R-CRT-EGFP or E1V-CRT-EGFP suggests that the isoforms are subject to different proteasomal mechanisms. We, therefore, examined the possible involvement of the Ub-proteasome system in these differences. CHO cells were co-transfected to express HA epitope-tagged Ub and either R-CRT or E1V-CRT, and ubiquitination status was examined. Six hours after co-transfection, cells were incubated with MG132 for 18 h to allow accumulation of Ub conjugates. R-CRT-EGFP and E1V-CRT-EGFP were then immunoprecipitated from lysed cells with anti-GFP Ab (Fig. 10*A*) and analyzed by Western blotting with anti-HA Ab. HA-Ub conjugates were detected only for R-CRT (Fig. 10*B*), suggesting that arginylation is necessary for an efficient ubiquitination of R-CRT and that non-arginylatable CRT is degraded via a Ub-independent proteasomal pathway.

Why Does Arginylation of CRT Not Follow the N-end Rule?—According to the N-end rule, Arg is a primary destabilizing residue that targets proteins for degradation by the Ub-protea-

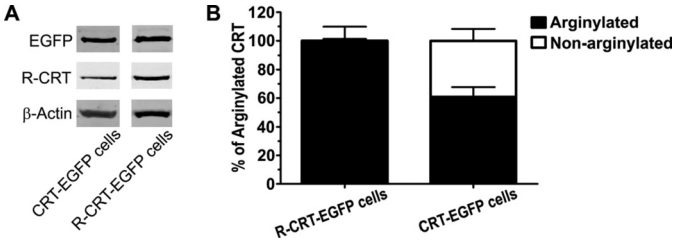

FIGURE 7. **Proportion of R-CRT in CRT-EGFP cells.** *A*, stably transfected cells expressing CRT-EGFP and R-CRT-EGFP were treated with MG132 (10 μM) for 12 h to cause accumulation of these proteins. MG132 was removed, and cells were washed 4 times, cultured for 1 h to allow diffusion of the inhibitor, washed again, and incubated for 2 h in presence of CHX. CRT-EGFP and R-CRT-EGFP content was analyzed by immunoblotting using anti-GFP, anti-R-CRT, and anti-β-actin Abs. *B*, the fraction of R-CRT-EGFP present in CRT-EGFP cells was obtained from the relations between the intensities of EGFP and R-CRT bands and plotted as a percent of the relation between EGFP and R-CRT bands intensities in R-CRT-EGFP cells. The relation between the intensities of EGFP and R-CRT bands in R-CRT-EGFP cells reflects the different sensitivity of anti-GFP and anti-R-CRT Abs and corresponds to 100% of R-CRT-EGFP. The estimated non-arginylated CRT-EGFP in CRT-EGFP cells was 40%, corresponding to the point 2 h in the half-life determination experiments (Fig. 5). Data represent the mean ± S.E. of seven independent experiments.

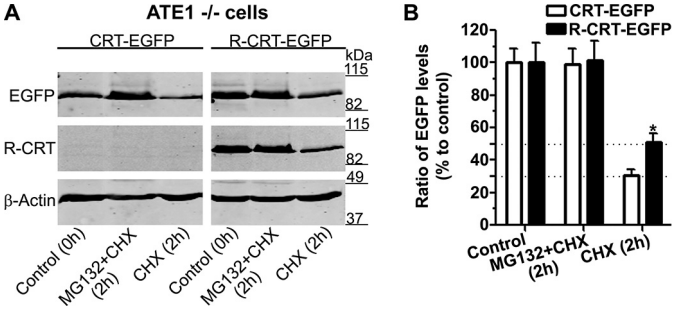

FIGURE 8. **Arginylation-independent proteasomal degradation of CRT.** Ate1$^{-/-}$ cells were transfected with Ub-CRT-EGFP or Ub-R-CRT-EGFP and treated with MG132 for 18 h to cause accumulation of CRT-EGFP or R-CRT-EGFP. MG132 was removed, and cells were incubated in the absence or presence of CHX or CHX+MG132 for 2 h. *A*, immunoblotting. *B*, intensities of EGFP bands relative to β-actin were measured and plotted as a percentage of initial band intensity (control: 0 h). Data are shown as the mean ± S.E. of three independent experiments. *, $p < 0.05$.

some system (19, 20). However, we found that the half-life of CRT, which has a Glu residue at its N terminus, is shorter than that of R-CRT. What is the cause of the higher half-life of R-CRT? We demonstrated previously that R-CRT but not CRT is recruited to SGs and that R-CRT moves to the plasma membrane in response to stress, acting as a pro-apoptotic signal (11). Arginylation may, therefore, protect CRT from proteasomal degradation under stress conditions by altering its metabolic fate. The dimerization of R-CRT is of a higher magnitude than that of CRT. Disulfide-bridged dimerization is essential for scaffolding of larger SGs under heat shock (13).

The above findings suggest that dimerization of R-CRT is another way to avoid proteasomal degradation. To evaluate this possibility, we examined R-CRT accumulation in cells incubated in the absence *versus* presence of (i) MG132 and (ii) dimerization conditions. Because homodimers of CRT are formed under non-reducing conditions by exposure of free SH-Cys-146 (13, 37, 38), we generated a CRT mutant (C146A-CRT-EGFP) that cannot dimerize. CRT knock-out fibroblasts (CRT$^{-/-}$) were transfected with C146A-CRT-EGFP or WT CRT (WT-CRT-EGFP) that are directed to the ER. Transfected cells were analyzed by immunocytochemistry using anti-R-CRT Ab (Fig. 11). Cells transfected with C146A-CRT and incubated in the absence of MG132 showed R-CRT levels 25% lower than those of cells transfected with WT-CRT-EGFP (Fig. 11, *A*, *B*, and *E*). R-CRT levels in MG132-treated cells were 2-fold higher than those in MG132-nontreated cells (Fig. 11*E*), regardless of the dimerization capability of the transfected protein. This finding is consistent with the idea that R-C146A-CRT remains in a monomeric form susceptible to proteasomal degradation. Similar results were obtained when NIH-3T3 cells were cultured in the presence of dithiothreitol to induce disulfide bridge breakage, and R-CRT levels were determined in the presence *versus* absence of MG132 (data not shown). These findings indicate that R-CRT dimerization prevents its proteasomal degradation and accounts for its reduced turnover rate (Fig. 5).

In summary, the dimerization capability of different CRT isoforms is correlated with their susceptibility to proteasomal degradation. In contrast to the N-end rule, which predicts a longer half-life for CRT than for R-CRT, our results indicate that CRT arginylation is responsible for the longer half-life of R-CRT, even though this isoform is the substrate of the Ub-proteasome system.

Discussion

The present study was focused on the degradation mechanism whereby cells modulate cytoplasmic CRT and R-CRT levels. Our previous studies have shown that R-CRT is directed to SG under stress conditions in which Ca^{2+} levels are decreased (7, 12, 39) and that R-CRT may reach the plasma membrane if the stress persists (11). It was suggested that CRT from plasma membrane is degraded in the lysosome pathway (40). However, the degradation pathway of internal CRT is unclear, and that of R-CRT is completely unknown. Afshar *et al.* (24) claimed that cyt-CRT is not a proteasomal substrate because it did not detect ubiquitinated cyt-CRT in cells. On the other hand, Labriola *et al.* (25) suggested that CRT is degraded in the cytosol by proteasome because, after exposure of cells to an inhibitor of ER Ca^{2+}-ATPase, cyt-CRT level was reduced by CHX treatment and increased by MG132 treatment. Our present findings indicate that both CRT and R-CRT are proteasomal substrates, although the degradation rate of R-CRT is lower than that of CRT (Figs. 4, 5, 8, and 9). The same trend was observed for the endogenous protein (Figs. 1 and 2), indicating that R-CRT half-life is not affected by other PTMs on CRT after passage through the ER.

R-CRT accumulation in cells is a consequence of proteasome inhibition (Figs. 1 and 2). Such accumulation occurs primarily during the first hour of MG132 exposure, suggesting that cyt-CRT is regulated at the retrotranslocation level. Our findings show clearly that the accumulation is due to blocking of proteasomal activity rather than to increased retrotranslocation or CRT synthesis (Fig. 1, *C* and *D*), consistent with previous findings that CRT retrotranslocation is independent of proteasomal activity (24). ER stress does not appear to promote R-CRT accumulation, because MG132 treatment of cells produced only a slight accumulation of reporter cytoplasmic substrates (41).

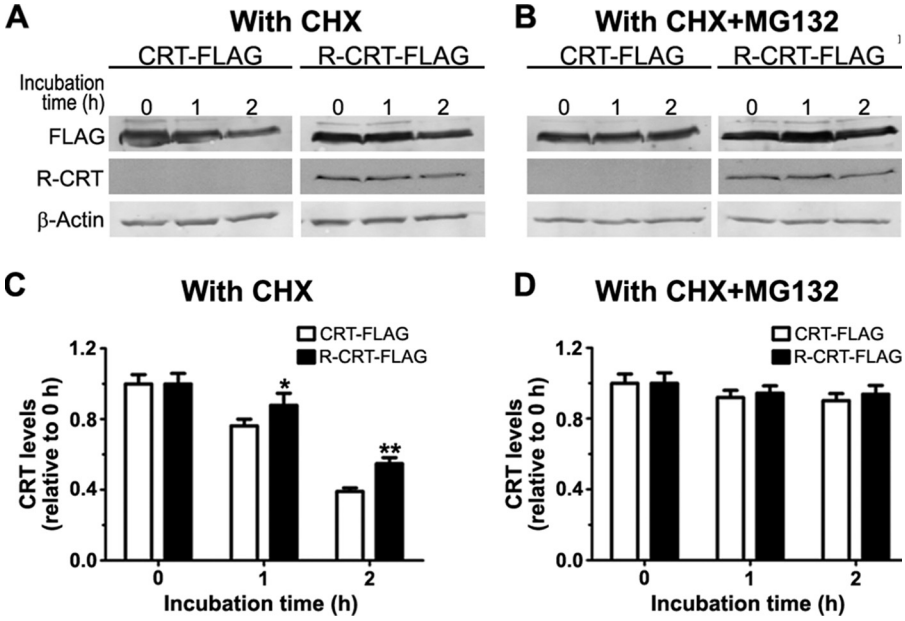

FIGURE 9. **EGFP does not contribute to proteasomal degradation of CRT fusion proteins.** Ate1$^{-/-}$ cells were transfected with Ub-CRT-FLAG or Ub-R-CRT-FLAG and treated with MG132 for 12 h to cause accumulation of CRT-FLAG or R-CRT-FLAG. MG132 was removed, cells were incubated in the absence or presence of CHX (*A*) or CHX+MG132 (*B*) for 1 or 2 h, and proteins were separated and immunoblotted. *C*, intensities of FLAG bands relative to β-actin were measured and plotted as a percentage of initial band intensity (control: 0 h). Data are shown as the mean ± S.E. of three independent experiments. *, $p < 0.05$; **, $p < 0.01$.

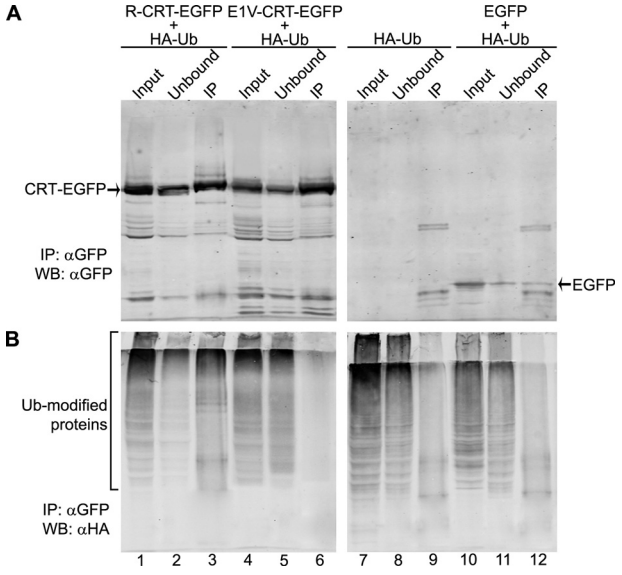

FIGURE 10. **R-CRT is ubiquitinated.** CHO cells were co-transfected with HA epitope-tagged Ub and Ub-R-CRT-EGFP or Ub-E1V-CRT-EGFP. Control cells were transfected with HA epitope-tagged Ub alone or with EGFP. Transfected cells were treated with MG132 for 18 h to cause accumulation of Ub conjugates, R-CRT-EGFP, or E1V-CRT-EGFP. Cell lysates were immunoprecipitated with anti-GFP Ab followed by immunoblotting (*WB*) with anti-GFP (*A*) and anti-HA (*B*) Abs. *Lanes 3*, *6*, *9*, and *12*, immunoprecipitated proteins (*IP*); *lanes 1*, *4*, *7*, and *10*, total cell lysate (*Input*): *lanes 2*, *4*, *8*, and *11*, flow-through (Unbound).

Arginylatable CRT, R-CRT isoform, and non-arginylatable mutant E1V-CRT expressed in cytoplasm had very different half-lives: longest for E1V-CRT (~4.8 h), intermediate for R-CRT (~2.0 h), and shortest for CRT (~0.7 h) (Fig. 5). R-CRT was ubiquitinated, but E1V-CRT was not (Fig. 10). These findings, taken together, could be interpreted as following the N-end rule, in that arginylation of proteins facilitated their recognition by E3 Ub ligases and was followed by proteasomal degradation (19, 20). However, ubiquitination in this case did not confer a shorter half-life to R-CRT as predicted by the N-end rule. Rather, our findings are consistent with proteasomal degradation of CRT by two distinct mechanisms, one Ub-dependent and the other Ub-independent. Similar results have been obtained for other proteins (*e.g.* ornithine decarboxylase, c-FOS, p21$^{Waf1/Cip1}$) that undergo proteasomal degradation in the absence of Ub modification (21, 42). However, it cannot be discarded that both isoforms of CRT could be degraded by the ubiquitin proteasome system with a difference in the efficiency of their ubiquitination. Further studies of the ubiquitination of R-CRT will be useful to elucidate the detailed mechanism of proteasomal targeting for its degradation.

The proteasomal pathway involves several coexisting types of proteasomes (26S, 20S, immunoproteasome, etc.) (43). 26S proteasomes, which account for ~15% of total proteasomes, degrade natively folded and functional proteins in a primarily Ub-dependent manner (43). In contrast, 20S proteasomes, which account for ~40% of total proteasomes, degrade damaged/misfolded proteins in a Ub-independent manner (43). Different proteasome complexes may, therefore, be responsible for the strikingly different half-lives of CRT, R-CRT, and E1V-CRT. Ubiquitinated R-CRT is most likely degraded by 26S proteasomes, whereas non-ubiquitinatable E1V-CRT is degraded by some other type. Because CRT can be arginylated by cellular Ate1, it may be degraded by more than one type of proteasomal complex, accounting for its lower half-life in cells that express CRT-EGFP. In Ate1$^{-/-}$ cells expressing CRT or R-CRT, degradation of the two proteins is related to differences in half-life similar to those observed in the other experimental systems used (Figs. 8 and 9). CRT expressed in Ate1$^{-/-}$ cells remains

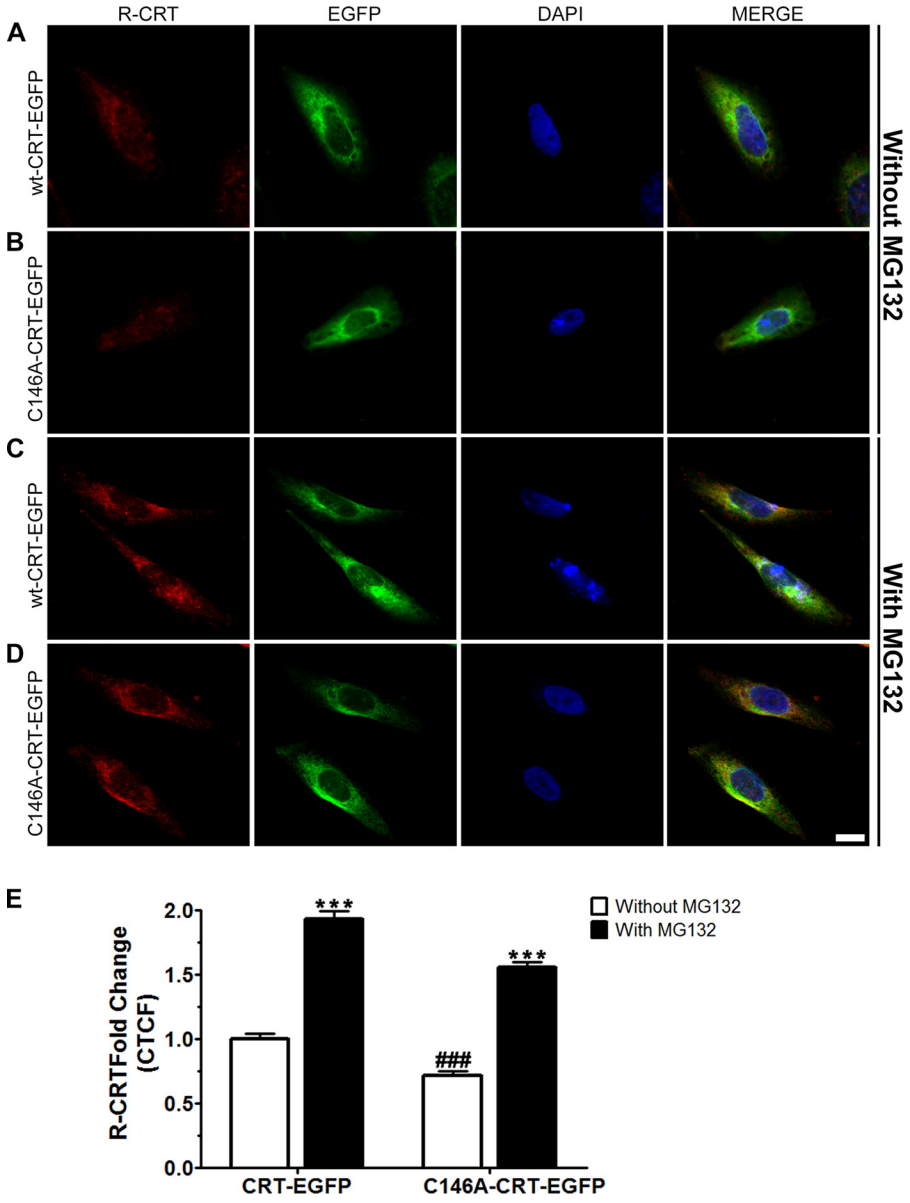

FIGURE 11. **R-CRT dimerization interferes with proteasomal degradation.** $CRT^{-/-}$ cells were transfected with WT-CRT-EGFP (*A* and *C*) or C146A-CRT-EGFP (*B* and *D*) and incubated in the absence (*A* and *B*) or presence (*C* and *D*) of MG132 for 2 h. *Scale bar*, 10 μm. Cells were analyzed as in Fig. 2. *E*, quantification of fluorescence intensity. Corrected total cell fluorescence is expressed as -fold change value relative to control (0 h). Data are shown as the mean ± S.E. ***, $p <$ 0.001 for intragroup comparison; *i.e. black bar versus white bar* within CRT-EGFP or C146A-CRT-EGFP group. ###, $p < 0.001$ for intergroup comparison; *i.e. white* or *black bar* of C146A-CRT-EGFP group *versus* the corresponding *bar* of CRT-EGFP group. Results are representative of 150 cells from at least three separate experiments for each condition.

arginylation-free, similarly to E1V-CRT expressed in stably transfected CHO cells. However, the half-life of the E1V-CRT isoform is longer than that of R-CRT (Fig. 5), suggesting that CRT turnover is altered by point mutation of the Glu residue.

In regard to the molecular determinants that target CRT to proteasomal degradation, we hypothesize that other PTMs such as phosphorylation (44) or the presence of PEST sequences in the CRT primary structure could be involved. Previous reports suggest that intrinsically disordered regions, unfolding, and oxidative damage are potential determinants of proteasomal degradation (21, 45). Further studies are needed to clarify the molecular contributions of such determinants to CRT degradation.

Arginylation of CRT affects its subcellular localization (7, 11). We observed that proteasomal inhibition resulted in accumulation of R-CRT in SGs (Fig. 1). Because only R-CRT is associated with SGs (7), we presume that these structures interfere with proteasomal degradation of R-CRT. Arginylation may also promote molecular rearrangements of the cyt-CRT population, *e.g.* by facilitating homodimer formation (13), and thereby block proteasomal degradation (Fig. 11). Important points remaining to be clarified are whether R-CRT is protected from degradation because the dimerized form cannot undergo polyubiquitination, or polyubiquitinated R-CRT is protected from degradation by physical association with stress granules.

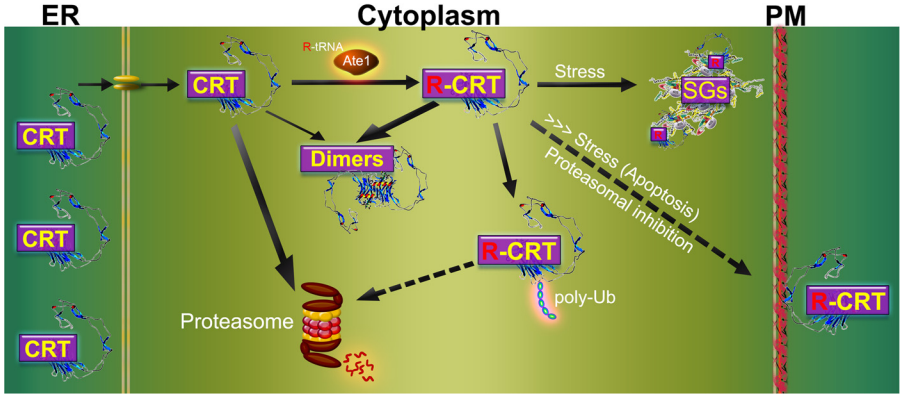

FIGURE 12. **Proposed model for differential fates of R-CRT and mechanism for cyt-CRT and R-CRT degradation.** The *arrow thickness* is proportional to efficiency of the process. CRT is synthesized in the ER, where its signal peptide is cleaved by peptide hydrolases to release the mature protein. CRT retrotranslocated to the cytoplasm is arginylated by Ate1 to generate R-CRT. Both isoforms can be degraded by proteasomes, but only R-CRT is ubiquitinated, suggesting that different proteasomal degradation mechanisms are involved. The CRT and R-CRT populations can be partially dimerized in different proportions. Under stress conditions, only R-CRT is recruited to SGs. When the stress exceeds a threshold value, R-CRT also appears in the plasma membrane. The indicated R-CRT locations are responsible for interfering with proteasomal degradation and increasing metabolic stability.

Previous studies indicate that proteins such as C/EBP are stabilized by homodimer or heterodimer formation (46). The longer half-life of R-CRT (Fig. 12) may result from any of the mechanisms mentioned above (ubiquitination, dimer formation, association with SGs, accumulation at the plasma membrane). Once CRT leaves the ER, it must be removed quickly from the cytoplasm because its continued presence would alter Ca^{2+} homeostasis so as to reduce cell survival. CRT is involved in a variety of injury processes including cell stress, apoptosis, and phagocytosis. CRT must be stabilized in the cytoplasm in order to play its normal role in these processes. Arginylation of CRT is important for such stabilization as well as for the processes of SG formation, plasma membrane localization, and pro-apoptotic signaling. The regulation of CRT levels in various subcellular structures depends on control of not only its synthesis (47) but also its degradation.

The present findings demonstrate cross-talk among the events of CRT retrotranslocation, post-translational arginylation, ubiquitination, and homodimer formation. Future studies will more fully elucidate the cross-talk among PTMs that modulate the fate of CRTs.

Acknowledgments—We are grateful to Drs. G. Pilar, B. L. Caputto, M. Galiano, B. Decca, M. Carpio, C. López-Sambooks, S. Durand, M. E. Carrizo, G. Nores, C. Argaraña, J. L. Barra, and H. Maccioni for helpful discussions, to G. Schachner, S. Deza, C. Sampedro, P. Abadie, P. Crespo, A. Comba, L. Bonnet, and C. Mas for technical assistance and to Dr. S. Anderson for English editing of the manuscript.

References

1. Walsh, C. T., Garneau-Tsodikova, S., and Gatto, G. J., Jr. (2005) Protein posttranslational modifications: the chemistry of proteome diversifications. *Angew. Chem. Int. Ed. Engl.* **44,** 7342–7372
2. Hallak, M. E., and Bongiovanni, G. (1997) Posttranslational arginylation of brain proteins. *Neurochem. Res.* **22,** 467–473
3. Saha, S., and Kashina, A. (2011) Posttranslational arginylation as a global biological regulator. *Dev. Biol.* **358,** 1–8
4. Ciechanover, A., Ferber, S., Ganoth, D., Elias, S., Hershko, A., and Arfin, S. (1988) Purification and characterization of arginyl-tRNA-protein transferase from rabbit reticulocytes: its involvement in post-translational modification and degradation of acidic NH2 termini substrates of the ubiquitin pathway. *J. Biol. Chem.* **263,** 11155–11167
5. Hu, R. G., Brower, C. S., Wang, H., Davydov, I. V., Sheng, J., Zhou, J., Kwon, Y. T., and Varshavsky, A. (2006) Arginyltransferase, its specificity, putative substrates, bidirectional promoter, and splicing-derived isoforms. *J. Biol. Chem.* **281,** 32559–32573
6. Wang, J., Han, X., Saha, S., Xu, T., Rai, R., Zhang, F., Wolf, Y. I., Wolfson, A., Yates, J. R., 3rd, and Kashina, A. (2011) Arginyltransferase is an ATP-independent self-regulating enzyme that forms distinct functional complexes *in vivo*. *Chem. Biol.* **18,** 121–130
7. Decca, M. B., Carpio, M. A., Bosc, C., Galiano, M. R., Job, D., Andrieux, A., and Hallak, M. E. (2007) Post-translational arginylation of calreticulin: a new isospecies of calreticulin component of stress granules. *J. Biol. Chem.* **282,** 8237–8245
8. Wong, C. C., Xu, T., Rai, R., Bailey, A. O., Yates, J. R., 3rd, Wolf, Y. I., Zebroski, H., and Kashina, A. (2007) Global analysis of posttranslational protein arginylation. *PLoS Biol.* **5,** e258
9. Karakozova, M., Kozak, M., Wong, C. C., Bailey, A. O., Yates, J. R., 3rd, Mogilner, A., Zebroski, H., and Kashina, A. (2006) Arginylation of β-actin regulates actin cytoskeleton and cell motility. *Science* **313,** 192–196
10. Zhang, F., Saha, S., and Kashina, A. (2012) Arginylation-dependent regulation of a proteolytic product of talin is essential for cell-cell adhesion. *J. Cell Biol.* **197,** 819–836
11. López Sambrooks, C., Carpio, M. A., and Hallak, M. E. (2012) Arginylated calreticulin at plasma membrane increases susceptibility of cells to apoptosis. *J. Biol. Chem.* **287,** 22043–22054
12. Carpio, M. A., López Sambrooks, C., Durand, E. S., and Hallak, M. E. (2010) The arginylation-dependent association of calreticulin with stress granules is regulated by calcium. *Biochem. J.* **429,** 63–72
13. Carpio, M. A., Decca, M. B., Lopez Sambrooks, C., Durand, E. S., Montich, G. G., and Hallak, M. E. (2013) Calreticulin-dimerization induced by post-translational arginylation is critical for stress granules scaffolding. *Int. J. Biochem. Cell Biol.* **45,** 1223–1235
14. Wang, W. A., Groenendyk, J., and Michalak, M. (2012) Calreticulin signaling in health and disease. *Int. J. Biochem. Cell Biol.* **44,** 842–846
15. Petris, G., Vecchi, L., Bestagno, M., and Burrone, O. R. (2011) Efficient detection of proteins retro-translocated from the ER to the cytosol by *in vivo* biotinylation. *PLoS ONE* **6,** e23712
16. Labriola, C. A., Giraldo, A. M., Parodi, A. J., and Caramelo, J. J. (2011) Functional cooperation between BiP and calreticulin in the folding maturation of a glycoprotein in *Trypanosoma cruzi*. *Mol. Biochem. Parasitol.* **175,** 112–117
17. Kwon, Y. T., Kashina, A. S., and Varshavsky, A. (1999) Alternative splicing results in differential expression, activity, and localization of the two forms of arginyl-tRNA-protein transferase, a component of the N-end rule path-

way. *Mol. Cell. Biol.* **19,** 182–193
18. Raghavan, M., Wijeyesakere, S. J., Peters, L. R., and Del Cid, N. (2013) Calreticulin in the immune system: ins and outs. *Trends Immunol.* **34,** 13–21
19. Tasaki, T., Sriram, S. M., Park, K. S., and Kwon, Y. T. (2012) The N-end rule pathway. *Annu. Rev. Biochem.* **81,** 261–289
20. Sriram, S. M., Kim, B. Y., and Kwon, Y. T. (2011) The N-end rule pathway: emerging functions and molecular principles of substrate recognition. *Nat. Rev. Mol. Cell Biol.* **12,** 735–747
21. Erales, J., and Coffino, P. (2014) Ubiquitin-independent proteasomal degradation. *Biochim. Biophys. Acta* **1843,** 216–221
22. Rechsteiner, M., and Hill, C. P. (2005) Mobilizing the proteolytic machine: cell biological roles of proteasome activators and inhibitors. *Trends Cell Biol.* **15,** 27–33
23. Gold, L. I., Eggleton, P., Sweetwyne, M. T., Van Duyn, L. B., Greives, M. R., Naylor, S. M., Michalak, M., and Murphy-Ullrich, J. E. (2010) Calreticulin: non-endoplasmic reticulum functions in physiology and disease. *FASEB J.* **24,** 665–683
24. Afshar, N., Black, B. E., and Paschal, B. M. (2005) Retrotranslocation of the chaperone calreticulin from the endoplasmic reticulum lumen to the cytosol. *Mol. Cell. Biol.* **25,** 8844–8853
25. Labriola, C. A., Conte, I. L., López Medus, M., Parodi, A. J., and Caramelo, J. J. (2010) Endoplasmic reticulum calcium regulates the retrotranslocation of *Trypanosoma cruzi* calreticulin to the cytosol. *PLoS ONE* **5,** e13141
26. Dantuma, N. P., Lindsten, K., Glas, R., Jellne, M., and Masucci, M. G. (2000) Short-lived green fluorescent proteins for quantifying ubiquitin/proteasome-dependent proteolysis in living cells. *Nat. Biotechnol.* **18,** 538–543
27. Ho, S. N., Hunt, H. D., Horton, R. M., Pullen, J. K., and Pease, L. R. (1989) Site-directed mutagenesis by overlap extension using the polymerase chain reaction. *Gene* **77,** 51–59
28. Hamalainen-Laanaya, H. K., and Orloff, M. S. (2012) Analysis of cell viability using time-dependent increase in fluorescence intensity. *Anal. Biochem.* **429,** 32–38
29. Laemmli, U. K. (1970) Cleavage of structural proteins during the assembly of the head of bacteriophage T4. *Nature* **227,** 680–685
30. Towbin, H., Staehelin, T., and Gordon, J. (1979) Electrophoretic transfer of proteins from polyacrylamide gels to nitrocellulose sheets: procedure and some applications. *Proc. Natl. Acad. Sci. U.S.A.* **76,** 4350–4354
31. Bogyo, M., and Wang, E. W. (2002) Proteasome inhibitors: complex tools for a complex enzyme. *Curr. Top. Microbiol. Immunol.* **268,** 185–208
32. Goll, D. E., Thompson, V. F., Li, H., Wei, W., and Cong, J. (2003) The calpain system. *Physiol. Rev.* **83,** 731–801
33. Bush, K. T., Goldberg, A. L., and Nigam, S. K. (1997) Proteasome inhibition leads to a heat-shock response, induction of endoplasmic reticulum chaperones, and thermotolerance. *J. Biol. Chem.* **272,** 9086–9092
34. Alvarez-Castelao, B., Martín-Guerrero, I., García-Orad, A., and Castaño, J. G. (2009) Cytomegalovirus promoter up-regulation is the major cause of increased protein levels of unstable reporter proteins after treatment of living cells with proteasome inhibitors. *J. Biol. Chem.* **284,** 28253–28262
35. Guo, N., and Peng, Z. (2013) MG132, a proteasome inhibitor, induces apoptosis in tumor cells. *Asia. Pac. J. Clin. Oncol.* **9,** 6–11
36. Kwon, Y. T., Kashina, A. S., Davydov, I. V., Hu, R. G., An, J. Y., Seo, J. W., Du, F., and Varshavsky, A. (2002) An essential role of N-terminal arginylation in cardiovascular development. *Science* **297,** 96–99
37. Jørgensen, C. S., Ryder, L. R., Steinø, A., Højrup, P., Hansen, J., Beyer, N. H., Heegaard, N. H., and Houen, G. (2003) Dimerization and oligomerization of the chaperone calreticulin. *Eur. J. Biochem.* **270,** 4140–4148
38. Rizvi, S. M., Mancino, L., Thammavongsa, V., Cantley, R. L., and Raghavan, M. (2004) A polypeptide binding conformation of calreticulin is induced by heat shock, calcium depletion, or by deletion of the C-terminal acidic region. *Mol. Cell* **15,** 913–923
39. Decca, M. B., Bosc, C., Luche, S., Brugière, S., Job, D., Rabilloud, T., Garin, J., and Hallak, M. E. (2006) Protein arginylation in rat brain cytosol: a proteomic analysis. *Neurochem. Res.* **31,** 401–409
40. Xiao, G., Chung, T. F., Fine, R. E., and Johnson, R. J. (1999) Calreticulin is transported to the surface of NG108–15 cells where it forms surface patches and is partially degraded in an acidic compartment. *J. Neurosci. Res.* **58,** 652–662
41. Menéndez-Benito, V., Verhoef, L. G., Masucci, M. G., and Dantuma, N. P. (2005) Endoplasmic reticulum stress compromises the ubiquitin-proteasome system. *Hum. Mol. Genet.* **14,** 2787–2799
42. Jariel-Encontre, I., Bossis, G., and Piechaczyk, M. (2008) Ubiquitin-independent degradation of proteins by the proteasome. *Biochim. Biophys. Acta* **1786,** 153–177
43. Tanahashi, N., Murakami, Y., Minami, Y., Shimbara, N., Hendil, K. B., and Tanaka, K. (2000) Hybrid proteasomes: induction by interferon-γ and contribution to ATP-dependent proteolysis. *J. Biol. Chem.* **275,** 14336–14345
44. Cristina Castañeda-Patlán, M., Razo-Paredes, R., Carrisoza-Gaytán, R., González-Mariscal, L., and Robles-Flores, M. (2010) Protein kinase C is involved in the regulation of several calreticulin posttranslational modifications. *Int. J. Biochem. Cell Biol.* **42,** 120–131
45. Ravid, T., and Hochstrasser, M. (2008) Diversity of degradation signals in the ubiquitin-proteasome system. *Nat. Rev. Mol. Cell Biol.* **9,** 679–690
46. Hattori, T., Ohoka, N., Inoue, Y., Hayashi, H., and Onozaki, K. (2003) C/EBP family transcription factors are degraded by the proteasome but stabilized by forming dimer. *Oncogene* **22,** 1273–1280
47. Nguyen, T. O., Capra, J. D., and Sontheimer, R. D. (1996) Calreticulin is transcriptionally upregulated by heat shock, calcium, and heavy metals. *Mol. Immunol.* **33,** 379–386